Chemistry–A European Journal
Research Article
doi.org/10.1002/chem.202402004
Chemistry Europe
European Chemical Societies Publishing
www.chemeurj.org

# Fluorinated Linkers Enable High-Voltage Pyrrolidinium-based Dicationic Ionic Liquid Electrolytes

Zviadi Katcharava[+],[a] Farahnaz Navazandeh-Tirkalaee[+],[a] Torje E. Orlamünde,[a] Karsten Busse,[a] Simon-Johannes Kinkelin,[b] Mario Beiner,[c] Anja Marinow,*[a] and Wolfgang H. Binder*[a]

Novel fluorinated, pyrrolidinium-based dicationic ionic liquids (FDILs) as high-performance electrolytes in energy storage devices have been prepared, displaying unprecedented electrochemical stabilities (up to 7 V); thermal stability (up to 370 °C) and ion transport (up to 1.45 mS cm$^{-1}$). FDILs were designed with a fluorinated ether linker and paired with TFSI/FSI counterions. To comprehensively assess the impact of the fluorinated spacer on their electrochemical, thermal, and physico-chemical properties, a comparison with their non-fluorinated counterparts was conducted. With a specific focus on their application as electrolytes in next-generation high-voltage lithium-ion batteries, the impact of the Li-salt on the characteristics of dicationic ILs was systematically evaluated. The incorporation of a fluorinated linker demonstrates significantly superior properties compared to their non-fluorinated counterparts, presenting a promising alternative towards next-generation high-voltage energy storage systems.

## Introduction

Hydrophobic, air-stable ILs have emerged as versatile electrolyte materials in a diverse array of electrochemical devices, including lithium ion batteries,[1] other metal batteries,[2] supercapacitors,[3] electrochemical actuators,[4] solar cells.[5] These electrochemical applications demand high ionic conductivity as well as robust chemical, thermal, and electrochemical stability. Particularly, pyrrolidinium-based ionic liquids have emerged as a promising alternative for electrochemical applications, due to their enhanced electrochemical and thermal stability.[6]

Dicationic ILs (DILs), also termed gemini-ILs are recently emerging, containing two cationic groups connected *via* a spacer/linker chain.[7] Compared to conventional ILs, DILs offer significantly more options (other than the choice of cations/anions) to tune properties by varying the spacer (link between two cations) length and its chemical nature. Various DILs based on imidazolium, pyrrolidinium and other common types of cations have been reported,[8] all containing non-fluorinated linkers, leaving the unexplored area and potential for further enhancing properties. Thus, dicationic pyrrolidinium and piperidinium bis(trifluoromethane)sulfonimide ionic liquids[8c] exhibit high electrochemical stability windows of up to 6.0 V vs. Li/Li$^+$ and high thermal stabilities up to ~300 °C doped with 1M LiTFSI. Imidazolium-based dicationic ILs have been evaluated as potential electrolytes, demonstrating ion conductivities up to 1.02 mS cm$^{-1}$ at 30 °C and electrochemical stability window up to 5.3 V.[8f]

We here present a novel fluorinated ionic liquid concept (FDIL) bridging pyrrolidinium-based ILs by fluorinated segments to combine the advantages of the fluorinated ether compounds with the unparalleled properties of pyrrolidinium-based ILs (see Figure 1). Fluorine-containing building blocks, in particular inside organic electrolytes, have emerged as an attractive molecular tool to address challenges associated with achieving key metrics such as high-energy density, cycle life, safety, and sustainability.[9] This is attributed to the hydrophobicity, robust bond strength, stability, and favorable dielectric properties of fluorine.[10] It is known that incorporation of fluorine enhances the performance of battery components by imparting them with high thermal and oxidative stability, chemical inertness, and non-flammability.[11] Fluorinated materials also play a vital role in facilitating the formation of a protective solid interface layer (SEI) at the metal-electrolyte interface, effectively preventing further chemical decomposition of the electrolyte.[12] Depending on specific requirements, fluorine-containing compounds find applications across various battery components, serving as liquid electrolytes, components of solid or gel

[a] Z. Katcharava,[+] F. Navazandeh-Tirkalaee,[+] T. E. Orlamünde, K. Busse, A. Marinow, W. H. Binder
Macromolecular Chemistry, Division of Technical and Macromolecular Chemistry, Faculty of Natural Sciences II (Chemistry, Physics, Mathematics), Institute of Chemistry, Martin-Luther University Halle-Wittenberg, von-Danckelmann-Platz 4, D-06120 Halle, Germany
E-mail: anja.marinow@chemie.uni-halle.de
wolfgang.binder@chemie.uni-halle.de

[b] S.-J. Kinkelin
Division of Technical Chemistry, Faculty of Natural Sciences II (Chemistry, Physics, Mathematics), Martin-Luther University Halle-Wittenberg, von-Danckelmann-Platz 4, D-06120 Halle, Germany

[c] M. Beiner
Fraunhofer Institute for Microstructure of Materials and Systems IMWS, Walter Hülse Str. 1, D-06120 Halle (Saale), Germany

[+] Z. K. and F. N.-T. contributed equally to this work.

Supporting information for this article is available on the WWW under https://doi.org/10.1002/chem.202402004

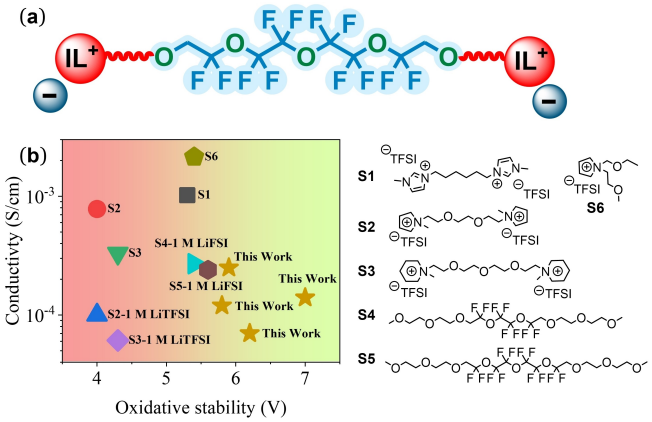


**Figure 1.** a) Schematic structure of dicationic ionic liquid with fluorinated linker and b) ionic conductivity (at 25–30 °C) vs. oxidative stability of relevant ionic liquids and fluorinated compounds.[8c,13]

electrolytes, salts, functional additives, separators, or protective coatings for electrodes.[10] Similar to conventional liquid electrolytes, the fluorination of the ILs may induce favorable properties, potentially enhancing segregation by forming additional fluorinated domains.[14] This ionic clustering and self-aggregation within IL can contribute to an elevation in ionic conductivity, with the added possibility that the fluorinated domains might further stabilize the SEI layer, rendering them suitable for applications as valuable electrolytes.[15]

Thus, the combination of the DIL-concept with perfluorinated middle segments is envisioned here as unexplored area of molecular diversity. The here prepared dicationic ionic liquids combine fluorinated ether chains as their middle segment (FDILs) and are compared to their non-fluorinated counterparts (see Figure 1). Similar to non-ionic fluorinated ether electrolytes, containing hydrofluoroethers displaying enhanced oxidative and thermal stabilities,[13b] we designed the perfluorinated ethereal building blocks to generate enhanced oxidative and thermal stabilities, herein reaching electrochemical stabilities of up to 7 Volts. Furthermore, our FDIL-concept bridges pyrrolidinium-based ILs by the now fluorinated segments, to combine the advantages of the fluorinated ether compounds with the favorable properties of pyrrolidinium-based ILs like low volatility, non-flammability, good solubility of salts, and high ionic conductivity.[5a,16] Choice of the counterions was based on bis(fluorosulfonyl)imide (FSI) and bis(trifluoromethylsulfonyl)imide (TFSI), due to their favorable thermal and electrochemical properties.[17] The synthesized dicationic ILs underwent comprehensive investigation to access their physical, organizational, thermal and electrochemical properties, with a focus on evaluating the impact of fluorination. Additionally, in a view toward their potential application as advanced electrolytes in next-generation batteries, we systematically studied the influence of added salt on the features of these novel dicationic ILs.[5a,16a,b]

## Results and Discussion

Scheme 1 outlines the synthetic route of the novel fluorinated dicationic ionic liquids (FDILs) and their non-fluorinated counterparts (DILs). Initially, N-methylpyrrolidium bromide (**IL-1**) was synthesized through quaternization of N-methyl-pyrrolidine with 1,6-dibromohexane. For FDILs, the subsequent step involved deprotonating fluorinated tetraethylene glycol (**FTEG**) with cesium carbonate in THF, followed by the addition of **IL-1** to the solution to yield fluorinated dicationic ionic liquid (**FDIL-1**). However, for non-fluorinated DILs, cesium carbonate proved ineffective for deprotonation, prompting a switch to sodium hydride. Therefore, predried tetraethylene glycol (**TEG**) was then deprotonated using NaH in THF, followed by addition of **IL-1** to produce **DIL-1**. Finally, a straightforward anion exchange was performed using either lithium bis(trifluoromethanesulfonyl)imide (LiTFSI) or lithium bis(fluorosulfonyl)imide (LiFSI), to obtain the respective final products: **FDIL-2**, **FDIL-3**, **DIL-2** and **DIL-3**. The details on synthetic procedure can be found in Supporting Information.

The structure of prepared pyrrolidinium-based dicationic ionic liquids was confirmed *via* $^{1}H$, $^{13}C$ and $^{19}F$ NMR spectroscopy (for spectra see Figures S1–S3). All compounds showed the expected resonances in NMR-spectroscopy. In Figure 2, the corresponding NMR spectra of **FDIL-2** are presented. The successful modification of the **FTEG** chains was confirmed by the proton signals of $CH_2$-groups at 4.01 and 3.56 ppm, respectively. The pyrrolidinium cations were identified by the signal of $CH_3$-group at 2.95 ppm, as well as the corresponding proton signals of $CH_2$-groups in the range of 3.49–3.35 ppm and at 2.06 ppm, respectively. The presence of the TFSI anion was confirmed through the characteristic signals observed between

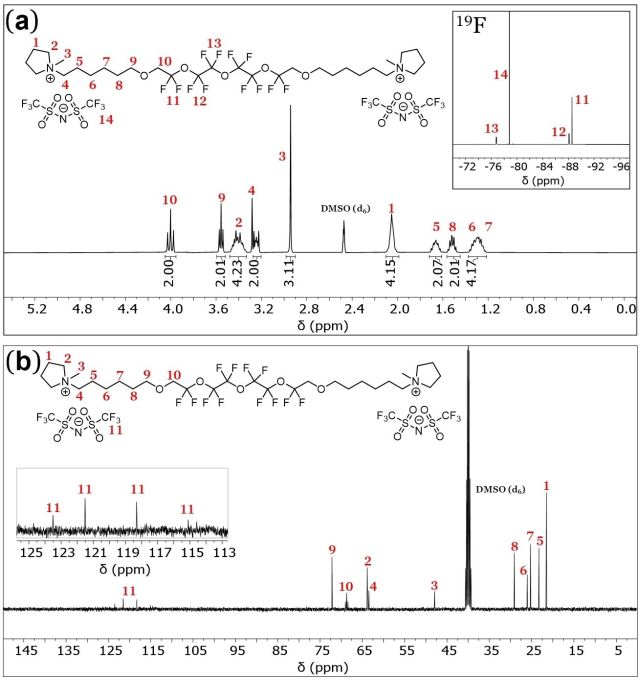


**Figure 2.** a) $^{1}H$ NMR ($^{19}F$ in insert), b) $^{13}C$ NMR spectrum of **FDIL-2** in DMSO–$d_6$.

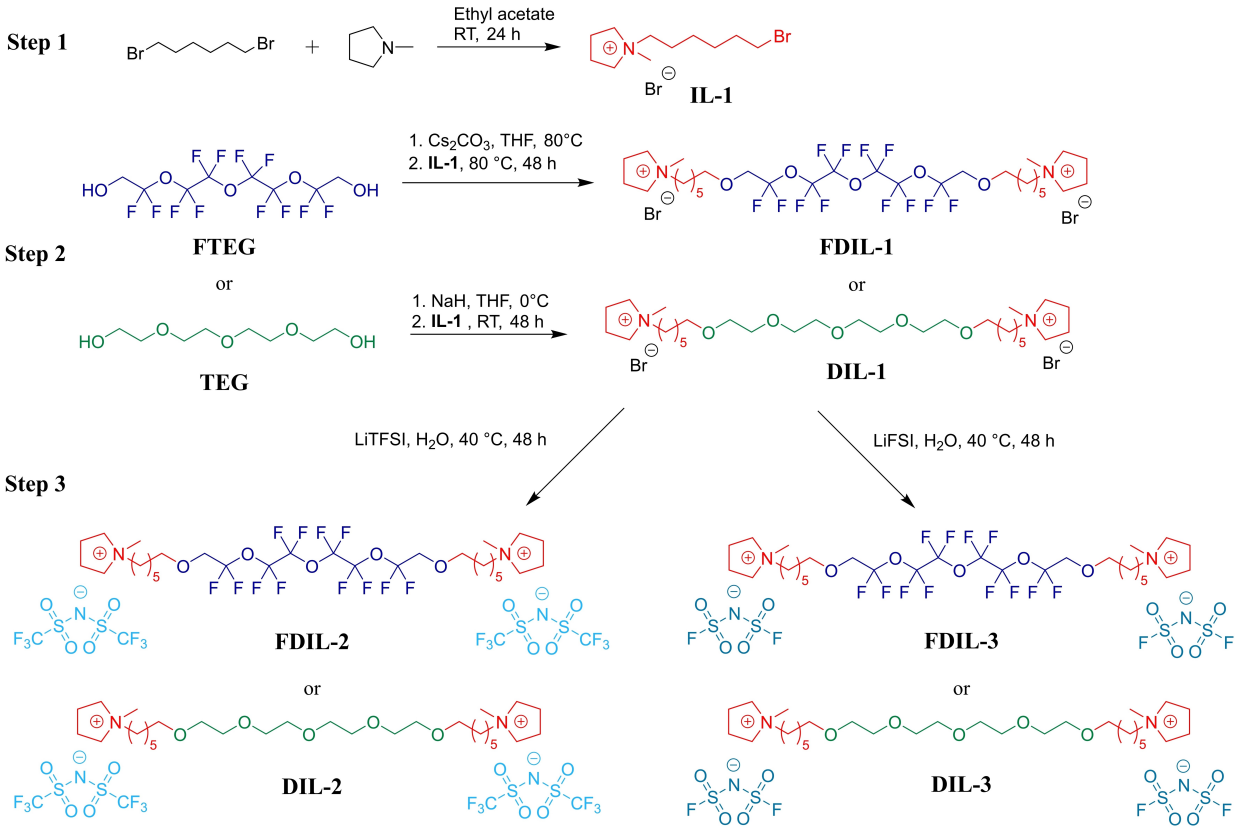


**Scheme 1.** Synthesis route of fluorinated and non-fluorinated dicationic ionic liquids.

125–115 ppm in the $^{13}$C-NMR spectrum (Inset in Figure 1b), and around −79 ppm in corresponding $^{19}$F-NMR spectrum (Inset Figure 1a). Additionally, characteristic signals of **FTEG** chain were identified in the $^{19}$F-NMR spectrum (Inset Figure 1a).

The prepared ILs could be further characterized *via* electrospray ionization mass spectrometry (ESI-MS), both in the positive and negative mode. Figure 3 Illustrates the expansion of the selected signals of fluorinated dicationic ILs **FDIL-2** and **FDIL-3** in positive and negative mode using [$C^{2+}$, 2 $A^-$] as notation for the neutral ionic liquid molecule. The comparison to the simulated isotopic pattern proves the accuracy of the assignments. The main species in the positive mode can be identified as [$C^{2+}$, $A^-$]$^+$, whereas the corresponding triplet anion species [$C^{2+}$, 3 $A^-$]$^-$ can be observed in negative mode.

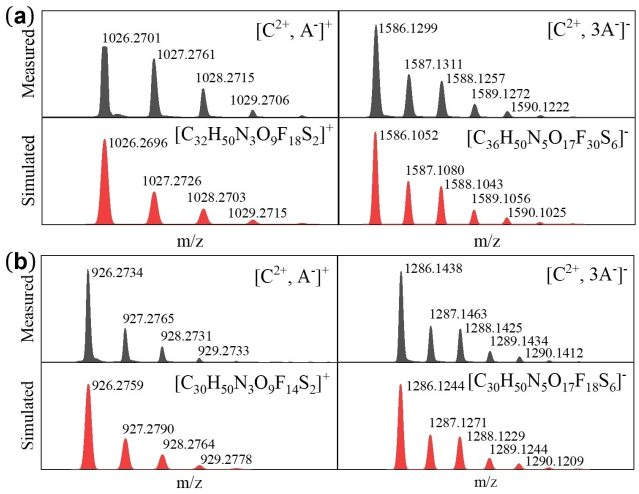


**Figure 3.** Expansion of selected ESI-MS signals in positive and negative mode of FDILs a) **FDIL–2** and b) **FDIL-3** and their corresponding isotopic pattern simulations.

In the context of their application as electrolytes, the physico-chemical properties of both the fluorinated and non-fluorinated dicationic ionic liquids are summarized in Table 1.

As thermal stabilities represent a key criterion for high temperature applications, thermogravimetric analysis (TGA) of the prepared DILs was conducted (Figure 4a), indicating a single decomposition step with onset decomposition temperatures ($T_d$) ranging between 244 and 370 °C for FDILs and 220–300 °C for DILs (see Table 1 and Figure 4a). The incorporation of the strong fluorine-carbon bonds significantly enhances thermal stability of the fluorinated compounds compared to their non-fluorinated counterparts,[13b] evident in Table 1, where fluorination led to a $T_d$ increase of 70 °C for TFSI-based ILs and approximately 24 °C for the FSI-based ones. Additionally, when comparing the influence of anions, the TFSI-containing ILs demonstrate significantly higher thermal stability compared to their FSI-containing counterparts due to the higher nucleophilicity of the FSI anion in-line with previous observations.[13b,18]

Controlling the glass transition-temperature ($T_g$) in ionic liquids is crucial in reaching high conductivity at ambient

**Table 1.** Physico-chemical properties of dicationic ionic liquids.

| Sample | Viscosity (cP) | | Decomposition temp. $T_d$ (°C) | Glass transition temp. $T_g$ (°C) | Oxidative decomposition voltage (V) | Conductivity (mS cm$^{-1}$) | | $Li^+$ Diffusivity ($10^{-6}$ cm$^2$/s) |
|---|---|---|---|---|---|---|---|---|
| | 30 °C | 70 °C | | | | 30 °C | 70 °C | |
| FDIL-2 | 1292 | 167 | 370 | −63 | 7.00 | 0.14 | 0.95 | |
| FDIL-2 + 1.0 M LiTFSI | 8801 | 577 | | | 5.75 | 0.02 | 0.24 | 2.66 |
| FDIL-3 | 1166 | 181 | 244 | −72 | 5.90 | 0.25 | 1.45 | |
| FDIL-3 + 1.0 M LiFSI | 1530 | 219 | | | 4.60 | 0.13 | 1.00 | 1.49 |
| DIL-2 | 4341 | 300 | 300 | −42 | 6.20 | 0.07 | 0.68 | |
| DIL-2 + 1.0 M LiTFSI | 10025 | 573 | | | 5.50 | 0.01 | 0.23 | 2.48 |
| DIL-3 | 2531 | 265 | 220 | −51 | 5.80 | 0.12 | 0.88 | |
| DIL-3 + 1.0 M LiFSI | 4460 | 419 | | | 5.60 | 0.08 | 0.84 | 2.48 |

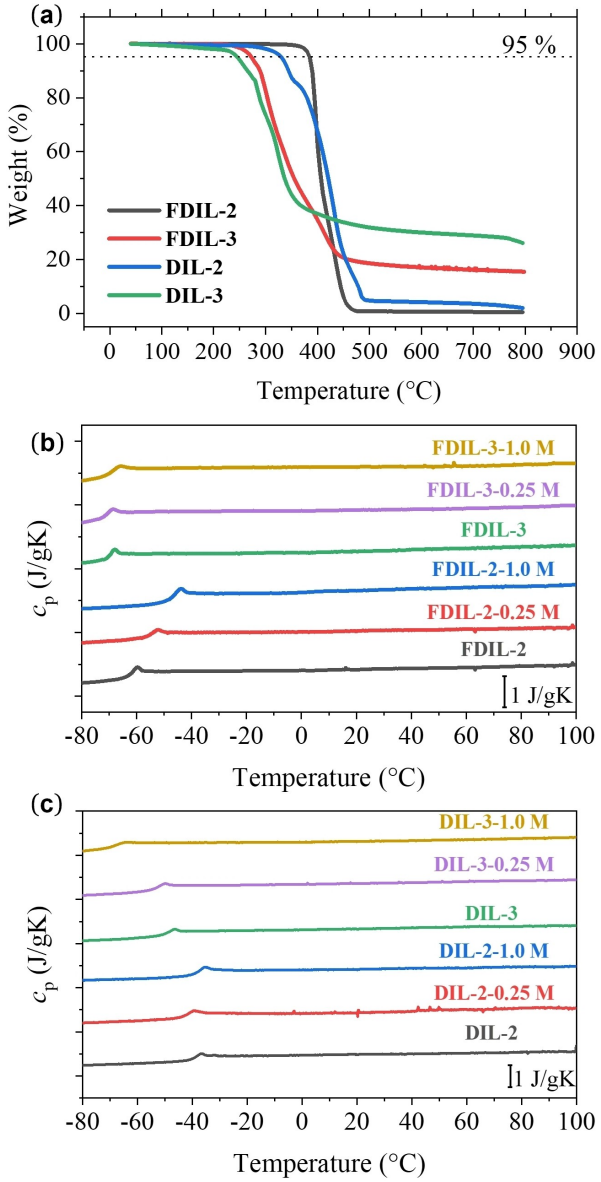


**Figure 4.** a) TGA of the prepared dicationic ILs, DSC thermograms of b) fluorinated DILs **FDIL-2** and **FDIL-3** before and after addition of the corresponding Li-salt, c) non-fluorinated DILs **DIL–2** and **DIL-3** before and after addition of the corresponding Li-salt.

temperatures due to coupling of ion transport to the molecular dynamics of the IL, described by the Vogel-Fulcher-Tammann (VFT)-behavior.[19] The influence of fluorination on the glass transition temperatures of the FDILs/DILs was measured by differential scanning calorimetry (DSC) (Table 1), proving that fluorination led to a significant decrease in glass transition temperatures, observing values of −63 °C and −72 °C for **FDIL-2** and **FDIL-3**, respectively. In contrast, $T_g$ ranged from −42 °C to −51 °C for **DIL-2** and **DIL-3**, respectively (see Table 1 and Figure 4). As expected, the presence of FSI anion led to an average decrease in $T_g$ of approximately 10 °C compared to the TFSI counterparts.

To get a clearer picture about ion transport-abilities both, FDILs and DILs were characterized by Broadband Dielectric Spectroscopy (BDS). In Figure 5a the conductivity of pure dicationic ILs is plotted as a function of inverse temperature. Introducing the fluorinated linker positively impacts the conductivity, with **FDIL-3** and **FDIL-2** (0.25 and 0.14 mS cm$^{-1}$ at 30 °C, respectively) outperforming **DIL-3** and **DIL-2** (0.12 and 0.02 mS cm$^{-1}$ at 30 °C, respectively) (see also Table 1). Additionally, using FSI as counterion further enhances the ionic transport properties (**FDIL-3** vs. **FDIL-2** and **DIL-3** vs. **DIL-2**, Table 1). The obtained values for non-fluorinated DILs are comparable with values previously reported for other dicationic ILs evaluated as electrolytes.[8c,f] The conductivity of the here reported DILs increases in the order of **DIL-2** < **DIL-3** < **FDIL-2** < **FDIL-3** across the entire measured temperature range, following Vogel-Fulcher-Tammann model described by the equation $\sigma = \sigma_0 \exp[-B/(T-T_0)]$,[20] where $\sigma_0$ represents the constant pre-exponential factor, B donates the constant related to energy, and $T_0$, also known as Vogel temperature, typically lies 50 °C below experimental $T_g$. The best-fit parameters are presented in Table 2. Vogel temperature values align with the order of the experimental $T_g$ values, indicating the highest pre-exponential factor $\sigma_0$ value for **FDIL-3**, consistent with experimentally obtained values. Conductivity behavior is strongly related to the viscosity of the material, with lower viscosity values significantly enhancing the ion transport properties of the material (Figure 5b, Table 1). Both the introduction of the fluorinated ether linker, as well as the switch to the significantly smaller FSI anion[7,21] results in the significant decrease in

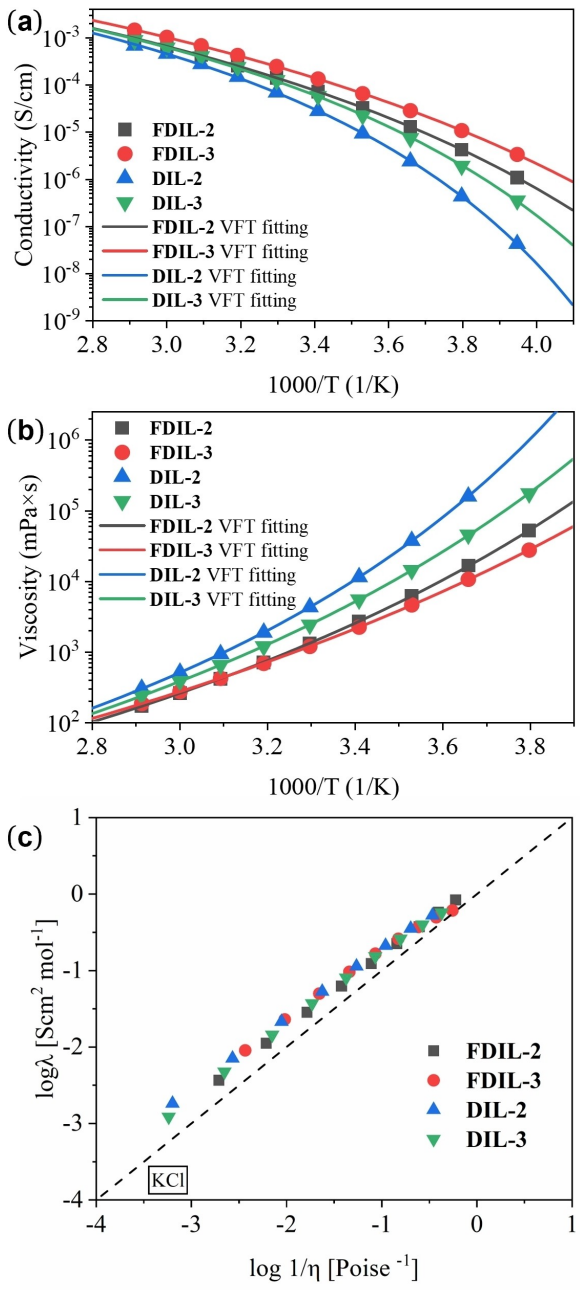


**Figure 5.** Plot of a) conductivity and b) viscosity as a function of temperature for the synthesized dicationic ionic liquids including corresponding VFT fit c) Walden plot of DILs.

**Table 2.** VFT equation parameters of ionic conductivity.

| Sample | $\sigma_0/10^{-1}$ (S/cm) | $B/10^3$ (K) | $T_0$ (K) | $R^2$ |
|---|---|---|---|---|
| FDIL-2 | 8.03 ± 0.83 | 1.20 ± 0.03 | 164.7 ± 1.26 | 0.9999 |
| FDIL-3 | 11.65 ± 1.17 | 1.26 ± 0.03 | 154.9 ± 1.4 | 0.9999 |
| DIL-2 | 4.86 ± 0.69 | 0.98 ± 0.03 | 193.2 ± 1.1 | 0.9999 |
| DIL-3 | 4.81 ± 1.19 | 1.00 ± 0.05 | 182.5 ± 2.5 | 0.9998 |

viscosity, thus improving conduction capabilities. The viscosity of the here reported ILs decreases in the order **DIL-2** > **DIL-3** > **FDIL-2** > **FDIL-3**, as well following VFT model (for fitting parameter see Table S1). As anticipated, the increase in temperature correlates with a reduction in viscosity, and consequently results in improved ion conductivity. Notably, ion conductivity reaching up to 1.5 mS cm$^{-1}$ was observed for **FDIL-3** at 70 °C (Table 1).

The Walden plot of the prepared fluorinated and non-fluorinated DILs is presented in Figure 5c, illustrating the relationship between molar conductivity (λ) and fluidity (1/η). Walden plot integrates data on density, viscosity, and conductivity to qualitatively access the ionicity of the ILs.[22] Ionicity provides valuable insights into transport properties, mobility and the potential formation of ionic aggregates, whose presence can decrease the mobility of ILs and increase their viscosity, leading to the behavior that deviates from that of an ideal electrolyte.[23] Thus, ionicity serves as a measure of aggregate formation, which is indicated by reduced fluidity and conductivity of the IL. The classification of ILs using the Walden plot as initially described by Angell and coworkers,[24] compares the data to an ideal reference electrolyte of aqueous KCl (0.01 mol/L), where ions are considered to be completely dissociated. As shown in Figure 5c, all four investigated DILs lie just above the ideal Walden line, indicating that they can be regarded as good ionic liquids with excellent transport properties, bordering on superionicity. Therefore, these strong ILs exhibit behavior similar to classical strong electrolytes in terms of ion association.[25] Interestingly, both fluorinated and non-fluorinated DILs exhibit similar behavior, falling in the same region of the Walden plot. This indicates the absence of fluorinated domains. Formation of such domains by the perfluorinated ethereal building blocks would hinder the independent movement of ionic components, thus resulting in lower ionicity.[26]

Electrochemical stability is a critical consideration in designing electrolytes for lithium batteries. The stability window of our **FDILs** and **DILs** was investigated *via* LSV measurements in the range from −8 V up to 8 V. As illustrated in Figure 6a, all investigated dicationic ILs exhibit a promisingly wide stability window. Both cathodic and anodic stability are in the range of −5 to −7 V, and 5 to 7 V, respectively. Furthermore, the beneficial effect of fluorination is evident when comparing **FDIL-2** to **DIL-2**. The introduction of a fluorinated linker in the DIL structure significantly enhances its oxidative stability (increase from 6 V for **DIL-2** to 7 V for **FDIL-2**, respectively). Similar trend is also observed in the case of the reductive stability (increase from −6 V for **DIL-2** to −7 V for **FDIL-2**, respectively). Moreover, the dicationic ILs are non-flammable, as demonstrated by a simple experiment comparing the burning behavior of **FDIL-2** and **DIL-2** -soaked paper (Figure 6c and d, respectively) to unsoaked paper (Figure 6b), clearly illustrating their non-flammable nature.

We further investigated the influence of salt concentration on the conductivity and viscosity of both fluorinated and non-fluorinated DILs. Varying amounts of a corresponding lithium salt, ranging from 0 M to 1.25 M (moles of salt per kg of IL), were added to the dicationic ILs. Figure 7 presents the obtained data, illustrating how viscosity and conductivity change with

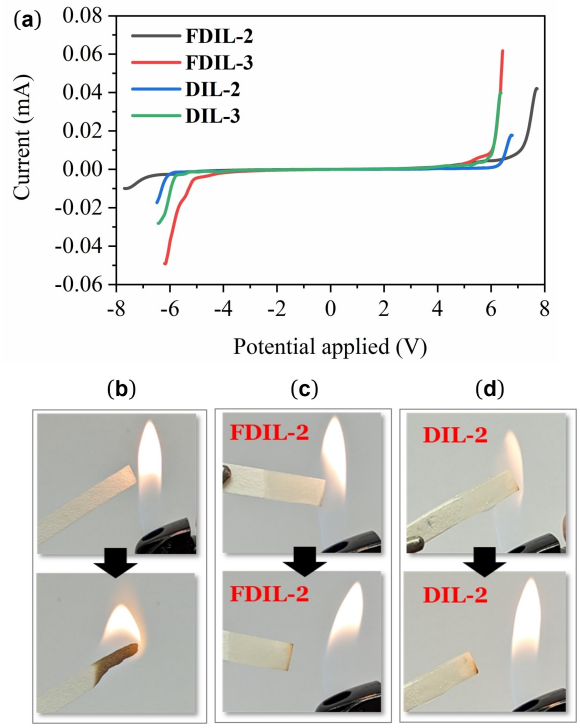


**Figure 6.** a) Electrochemical stability of the synthesized dicationic ionic liquids at room temperature, Flammability test b) untreated paper c) paper soaked with **FDIL-2**d) paper soaked with **DIL-2**.

temperature (see also Figures S4, S7–S10). Notably, the effect of salt concentration is most pronounced in **FDIL-2** (Figure 7a). The conductivity of **FDIL-2** decreases with increasing concentration of added lithium salt, with the effect particularly strong at the lower temperatures (Figure S4a). The reduction is presumably linked to the significant increase in viscosity with higher salt content, restricting the free movement of ions (Table S2).[27]

**FDIL-3** with FSI as counterion exhibits a weaker dependence on salt content as shown in Figure 7b, reaching conductivities of $10^{-3}$ S cm$^{-1}$ at 70 °C, dropping to $10^{-6}$ S cm$^{-1}$ at −20 °C. Using FSI as counterion noticeably reduces the viscosity of the FDIL across the entire temperature range, while the effect of the added salt was minimal. The viscosity of **FDIL-3** did not exceed $5\times10^{4}$ mPa s, while **FDIL-2** (1.25 M) reached $5\times10^{6}$ mPa s. The presence of the fluorinated linker in dicationic ILs additionally enhances the solubility of lithium salt, reaching 1.25 M in **FDIL-2** in comparison to **DIL-2** with 1.0 M. The behavior of **DIL-2** (Figure 7c) and **DIL-3** (Figure 7d) are similar to their fluorinated counterparts, and TFSI based samples display stronger dependence of both conductivity (Figure S4a and c) and viscosity on the concentration of added lithium salt.

Additionally, $^{7}$Li-diffusion coefficients for all ILs were determined via DOSY-NMR (see Table 1), obtaining $Li^{+}$-diffusion coefficients between 1.5 and $2.6\times10^{-6}$ cm$^2$/s (see S11, S12), which is a magnitude higher than the Li-diffusivity reported for pure fluorinated ether electrolytes,[13b] but comparable with values reported for other ILs.[27c,28] Glass transition-temperatures,

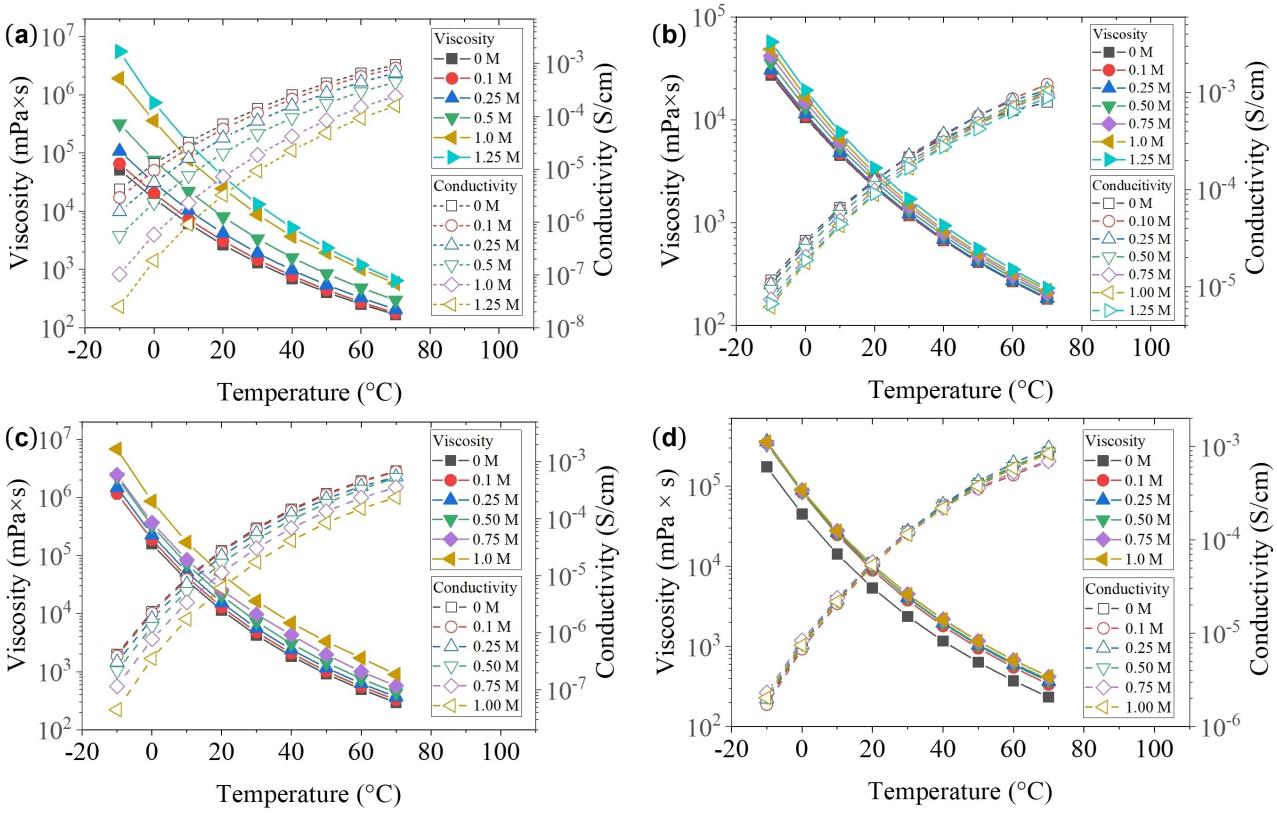


**Figure 7.** Conductivity and viscosity as a function of temperature for a) **FDIL-2**, b) **FDIL-3**, c) **DIL-2** and d) **DIL-3** with different salt concentrations.

$T_g$ are slightly enhanced (see Figure 4b and c) with increasing salt concentration for both, the fluorinated (**FDIL-2** and **FDIL-3**) and non-fluorinated ILs (**DIL-2** and **DIL-3**), in-line with literature.[28] It should be noted that the positive effect of fluorination on the electrochemical stability is also observable in the presence of additional salt when compared to the non-fluorinated ILs (see Figure S13).

As clustering effects of salt doping and changes in microstructure within ILs are a major factor in determining their application as electrolytes,[29] wide angle X-ray diffraction (WAXD) measurements were conducted. The WAXD patterns of pure FILs and samples with additional lithium salt are depicted in Figure 8a. Scattering vectors (q) are correlated to sizes of the heterogeneities by Bragg's law equation ($q = 4\pi sin\Theta/\lambda$). In Figure 8a, the main peak is observed at ~q = 13 $nm^{-1}$ (d = 0.483 nm) for both FILs, with an additional smaller peak at ~q = 8.5 $nm^{-1}$ (d = 0.739 nm) displaying higher intensity for **FIL-2** compared to the FSI containing one (**FIL-3**). For deconvolution of the observed peaks see Figure S5. It is assumed that higher q value corresponds to a charge ordering peak which is characteristic for ionic liquids, as previously reported by Ferreira *et al.*,[14b,30] closely linked to a scenario of nearest-neighbor distance, where ions are surrounded by counterions, ensuring local electroneutrality. Consistent with the observations from the Walden plot, there was no indication of the formation of fluorinated domains. The intensity and position of the main peak remain unaffected by the addition of Li salt. In contrast, a significant broadening of the second peak, observed at the lower q value, upon the addition of Li salt to FILs can be observed, possibly related to charge ordering, i.e., from the correlation of ions of the same charge (cation–cation and anion–anion). Upon salt addition, the peak significantly broadens, decreases in intensity and shifts to lower q values (from q = 8.3 to q = 6.9 $nm^{-1}$ for **FDIL-2** (d = 0.753 nm to d = 0.911 nm) and from q = 8.4 to q = 7.6 $nm^{-1}$ for **FDIL-3** (d = 0.748 nm to d = 0.826 nm), respectively), which is in accordance with previous results on ILs.[31] This may be an indication for the presence of LiTFSI/LiFSI clusters which leads to the increase of charge distance. In the case of non-fluorinated DILs (Figure 8b), a less pronounced ordering was observed. Interestingly, although ordering was observed for **DIL-2**, the exchange of the anion to the smaller FSI anion led to a significantly less pronounced internal ordering of **DIL-3** (Deconvolution of the observed peaks Figure S6). However, the addition of salt resulted in an almost disappearance of the second peak in both cases (**DIL-2** and **DIL-3**), indicating the absence of LiTFSI/LiFSI clusters in non-fluorinated ILs.

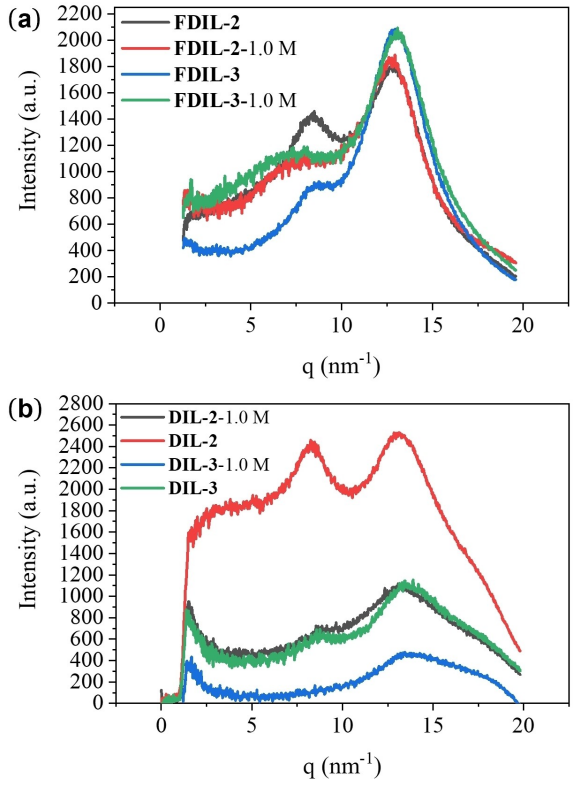


**Figure 8.** Wide angle X-ray diffraction (WAXD) measurements of a) **FDIL-2** and **FDIL-3** in pure form and after addition of the corresponding salt (1 M concentration), b) **DIL-2** and **DIL-3** in pure form and after addition of the corresponding salt (1 M concentration).

## Conclusions

Novel dicationic pyrrolidinium-based ionic liquids with aliphatic and fluorinated ether linkers paired with TFSI/FSI counterions have been synthesized and demonstrated to reach enhanced thermal and electrochemical stabilities due to the incorporation of the fluorinated middle-segment. The results highlight the beneficial impact of introducing a fluorinated linker into the DIL structure, significantly enhancing their properties and broadening their application potential. Fluorinated dicationic ILs **(FDILs)** exhibit exceptional oxidative stability, reaching up to 7 V, while displaying excellent thermal decomposition temperatures (up to 370 °C) and superior ionic conductivity (up to 1.45 mS $cm^{-1}$ at 70 °C). Furthermore, choice of the counterion in dicationic ILs allows for fine-tuning of properties according to specific application requirements. As the addition of Li-salt inside the FDILs does not lead to detrimental ion clustering effects but even enhanced Li-ion solubilities, the here prepared FDILs represent a novel class of electrolytes with enhanced stabilities, as needed for many electrochemical devices useful for charge-storage.

## Experimental Section

All used chemicals and instrumentation are described in the SI. Prior to the analysis, the water content of the prepared DILs was estimated by *Karl Fischer titration* using SI Analytics coulometer TitroLine 7500 KF trace. The water content was ranging from 50–100 ppm. *NMR spectroscopy:* $^{1}H$, $^{13}C$ and $^{19}F$ NMR were measured on a Varian FT-NMR spectrometer (400 and 101 MHz, respectively) (Agilent Technologies Germany GmbH & Co. KG, Waldbronn, Germany). $^{7}Li$ NMR spectra were recorded at 27 °C on a Agilent 500 MHz spectrometer with DD2 console, operating at 195.21 MHz for $^{7}Li$. *ESI-ToF-MS* was performed on a Bruker Daltonics microTOF via direct injection with a flow rate of 180 μL/h using the positive mode/negative mode. *TGA* was conducted using a Netzsch TG-209

F3 instrument. *ATR-IR spectra* were measured on a Bruker Tensor Vertex 70 equipped with a Golden Gate Heated Diamond ATR Top-plate. *DSC data* were collected using a PerkinElmer Pyris7. *BDS:* Novocontrol "Alpha analyzer" was used for investigating ionic conductivities. *Electrochemical characterization of the compounds by LSV* with 1 mV/s scan rate was conducted inside a glovebox (SylaTech GB 1200). For this purpose, the samples (10 mm diameter) were assembled into a Swagelok cell and contacted with two stainless steel stamps, which were mounted with a defined torque. An Autolab PGSTAT 204 with FRA32 M module by Metrohm running on Nova 2.1.5 Software was used as a potentiostat. *Viscosity measurements* were conducted on Anton Paar MCR-101 DSO rheometer equipped with cone-plate geometry (d = 25 mm). *Density measurements* were conducted on Anton Paar DMA 4200 density meter with temperature control. *Wide-angle X-ray diffraction (WAXD) measurements* were performed with an Incoatec (Geesthacht, Germany) IμS equipped with a microfocus source and a monochromator for CuKa radiation (lamda = 1.5406 Å).

The synthesis of both fluorinated (**FDILs**) and non-fluorinated (**DILs**) dicationic ionic liquid was performed in three stages (Scheme 1): alkylation, synthesis of a dicationic ionic liquid and anion exchange.

*Synthesis of **IL-1**:* Alkylation procedure was adapted from Liu et al.[32] Initially, 1,6-dibromohexane (18.0 mmol, 2.78 mL) was added to N-methylpyrrolidine (14.0 mmol, 1,45 mL) in 15 mL ethyl acetate in a round-bottom flask and stirred for 24 h at room temperature. Obtained white powder-like precipitate 1-(6-bromohexyl)-1-methyl-pyrrolidinium bromide (**IL-1**) was filtered, washed with ethyl acetate (3 times) and subsequently dried in high vacuum (0.01 mbar) over $P_2O_5$ for 48 h (Yield: 69 %).

*Synthesis of **FDIL-1**:* For deprotonation of fluorinated tetraethylene glycol (**FTEG**) a modified procedure previously described by Bao and coworkers[13b] was used. **FTEG** (4.4 mmol, 1.7 g) was dissolved in 50 mL dry THF in a two-neck round-bottom flask connected to a reflux condenser. Cesium carbonate ($Cs_2CO_3$, 2.5 eq., 11.0 mmol, 3.4 g), was separately dissolved in 50 mL dry THF and added to the flask. The suspension was stirred at 80 °C under reflux for 2 h. Then **IL-1** (2.2 eq. respective to **FTEG**, 9.7 mmol, 3.25 g) was added to the mixture and left for stirring at 80 °C under reflux for 48 h under nitrogen atmosphere. To extract **FDIL-1** the solvent was removed on rotary evaporator. The residue was dissolved in small amount of water (≈50 mL) and washed by diethyl ether (3×50 mL). The aqueous solution was collected and the product was *extracted* by dichloromethane (3×50 mL). The organic solution was dried with $Na_2SO_4$ and the solvent was removed by rotary evaporator (Yield: 75 %).

*Synthesis of **FDIL-2** and **FDIL-3**:* For an anion exchange reaction, **FDIL-1** (2.97 g, 3.3 mmol) was dissolved in 100 mL water, to which either lithium bis(trifluoromethanesulfonyl)imide (LiTFSI, 6.0 eq. 19.8 mmol, 5.7 g) or lithium bis(fluorosulfonyl)imide (LiFSI, 6.0 eq. 19.8 mmol, 3.7 g) was added to obtain **FDIL-2** and **FDIL-3**, respectively. The solution was stirred continuously at 40 °C for 48 h. Finally, fluorinated ionic liquid was extracted by DCM (3×50 mL) and the organic solution was washed with water (3×100 mL) to remove the residual Li-salts. The crude product was purified firstly *via* silica gel column chromatography. The obtained product was further purified by precipitating in diethyl ether. Finally, **FDIL-2** (Yield: 19 %) and **FDIL-3** (Yield: 22 %) were dried under high vacuum (0.01 mbar) over $P_2O_5$ for 48 h, and kept in the glove box for further use.

*Synthesis of **DIL-2** and **DIL-3**:* Tetraethylene glycol (**TEG**) was dried over molecular sieves (3 A°) prior to use. Sodium hydride (NaH, 3.0 eq. relative to **TEG**,13.2 mmol, 0.54 g) was dissolved in 100 mL dry THF in a two-neck round-bottom flask under nitrogen atmosphere in ice bath. Predried tetraethylene glycol (4.4 mmol, 0.77 mL) was dropwise added to the flask. The suspension was stirred at 0 °C for about 2 h. Then **IL-1** (2.2 eq. relative to **TEG**, 9.7 mmol, 3.25 g) was added to the mixture and left for stirring at room temperature for 48 h under nitrogen atmosphere. After reaction completion THF was removed *via* rotary evaporator and the residue was directly subjected to anion exchange. For an anion exchange reaction, **DIL-1** was dissolved in 100 mL water, to which either lithium bis(trifluormtheanesulfonyl)imide (LiTFSI, 6.0 eq. to the theoretical molar amount of **DIL-1**) or lithium bis(fluorosulfonyl)imide (LiFSI, 6.0 eq. to the theoretical molar amount of **DIL-1**) was added to obtain **DIL-2** and **DIL-3**, respectively. The solution was stirred continuously at 40 °C for 48 h. The non-fluorinated ionic liquid was extracted by DCM (3×50 mL) and the organic phase was washed with water (5×100 mL) to remove excessive reactants. Then the product was purified by silica gel column chromatography. Finally, **DIL-2** (Yield: 62 %) and **DIL-3** (Yield: 53 %) were dried under high vacuum (0.01 mbar) over $P_2O_5$ for 48 h, and kept in the glove box for further use.

## Supporting Information Summary

SI describes all experimental details (synthesis, analyses) and physical measurements. The authors have cited additional references within the Supporting Information.[13b,32]

## Acknowledgements

Authors acknowledge IoLiTec GmbH for providing lithium salts, Rene Sattler for conducting DSC measurements, Julian Radicke for providing density measurements and Dr. Dieter Ströhl for NMR measurements. This research was developed under the framework of the BAT4EVER project. This project has received funding from the European Union's Horizon 2020 research and innovation programme under grant agreement No 957225. WHB thanks the DFG project INST 271/444-1 FUGG for financial support; the DFG-Project BI1337/16-1; BI 1337/14-1 and the GRK 2670, W69000789, Project Nr. 436494874 for financial support. Open Access funding enabled and organized by Projekt DEAL.

## Conflict of Interests

The authors declare no conflict of interest.

## Data Availability Statement

The data that support the findings of this study are available in the supplementary material of this article.

**Keywords:** Ionic liquids 1 · Fluorinated materials 2 · Electrolytes 3 · Li-ion transport 4 · Oxidative stability 5

[1] a) M. Forsyth, L. Porcarelli, X. Wang, N. Goujon, D. Mecerreyes, *Acc. Chem. Res.* **2019**, *52*, 686–694; b) K. Liu, Z. Wang, L. Shi, S.

Jungsuttiwong, S. Yuan, *J. Energy Chem.* **2021**, *59*, 320–333; c) X. Tang, S. Lv, K. Jiang, G. Zhou, X. Liu, *J. Power Sources* **2022**, *542*, 231792.
[2] a) H. Zhang, L. Qiao, H. Kühnle, E. Figgemeier, M. Armand, G. G. Eshetu, *Energy Environ. Sci.* **2023**, *16*, 11–52; b) L. S. Domingues, H. G. de Melo, V. L. Martins, *Phys. Chem. Chem. Phys.* **2023**, *25*, 12650–12667; c) K. Sirengo, A. Babu, B. Brennan, S. C. Pillai, *J. Energy Chem.* **2023**, *81*, 321–338; d) B. Craig, T. Schoetz, A. Cruden, C. Ponce de Leon, *Renewable Sustainable Energy Rev.* **2020**, *133*, 110100.
[3] a) S. Pan, M. Yao, J. Zhang, B. Li, C. Xing, X. Song, P. Su, H. Zhang, *Front. Chem.* **2020**, *8*, 00261; b) J. Feng, Y. Wang, Y. Xu, Y. Sun, Y. Tang, X. Yan, *Energy Environ. Sci.* **2021**, *14*, 2859–2882; c) W. Xiong, Z. Yin, X. Zhang, Z. Tu, X. Hu, Y. Wu, *ACS Omega* **2022**, *7*, 26368–26374.
[4] a) S. Cao, J. Aimi, M. Yoshio, *ACS Appl. Mater. Interfaces.* **2022**, *14*, 43701–43710; b) J. C. Dias, D. M. Correia, C. M. Costa, C. Ribeiro, A. Maceiras, J. L. Vilas, G. Botelho, V. de Zea Bermudez, S. Lanceros-Mendez, *Electrochim. Acta* **2019**, *296*, 598–607.
[5] a) T. Zhou, C. Gui, L. Sun, Y. Hu, H. Lyu, Z. Wang, Z. Song, G. Yu, *Chem. Rev.* **2023**, *123*, 12170–12253; b) X. Li, C. Li, X. Zhao, Y. Zhang, G. Liu, Z. Zhang, D. Wang, L. Xiao, Z. Chen, B. Qu, *ACS Appl. Mater. Interfaces* **2021**, *13*, 4553–4559.
[6] a) F. Castiglione, M. Moreno, G. Raos, A. Famulari, A. Mele, G. B. Appetecchi, S. Passerini, *J. Phys. Chem. B* **2009**, *113*, 10750–10759; b) H. Qi, Y. Ren, S. Guo, Y. Wang, S. Li, Y. Hu, F. Yan, *ACS Appl. Mater. Interfaces* **2020**, *12*, 591–600; c) M. Kerner, P. Johansson, *Batteries* **2018**, *4*, 10.
[7] H. Niu, L. Wang, P. Guan, N. Zhang, C. Yan, M. Ding, X. Guo, T. Huang, X. Hu, *J. Energy Chem.* **2021**, *40*, 102659.
[8] a) J. L. Anderson, R. Ding, A. Ellern, D. W. Armstrong, *J. Am. Chem. Soc.* **2005**, *127*, 593–604; b) S. K. Singh, A. W. Savoy, *J. Mol. Liq.* **2020**, *297*, 112038; c) J. F. Velez, M. B. Vazquez-Santos, J. M. Amarilla, B. Herradon, E. Mann, C. del Rio, E. Morales, *J. Power Sources* **2019**, *439*, 227098; d) A. Zafar, T. Evans, R. G. Palgrave, I. ud-Din, *J. Chem. Res.* **2022**, *46*, 17475198221092966; e) F. Pandolfi, M. Bortolami, M. Feroci, A. Fornari, V. Scarano, D. Rocco, *Mater* **2022**, *15*, 866; f) T. C. Nirmale, N. D. Khupse, R. S. Kalubarme, M. V. Kulkarni, A. J. Varma, B. B. Kale, *ACS Sustainbale Chem. Eng.* **2022**, *10*, 8297–8304; g) J. F. Vélez, M. B. Vazquez-Santos, J. M. Amarilla, P. Tartaj, B. Herradón, E. Mann, C. del Río, E. Morales, *Electrochim. Acta* **2018**, *280*, 171–180.
[9] a) J. Amici, P. Asinari, E. Ayerbe, P. Barboux, P. Bayle-Guillemaud, R. J. Behm, M. Berecibar, E. Berg, A. Bhowmik, S. Bodoardo, I. E. Castelli, I. Cekic-Laskovic, R. Christensen, S. Clark, R. Diehm, R. Dominko, M. Fichtner, A. A. Franco, A. Grimaud, N. Guillet, M. Hahlin, S. Hartmann, V. Heiries, K. Hermansson, A. Heuer, S. Jana, L. Jabbour, J. Kallo, A. Latz, H. Lorrmann, O. M. Løvvik, S. Lyonnard, M. Meeus, E. Paillard, S. Perraud, T. Placke, C. Punckt, O. Raccurt, J. Ruhland, E. Sheridan, H. Stein, J.-M. Tarascon, V. Trapp, T. Vegge, M. Weil, W. Wenzel, M. Winter, A. Wolf, K. Edström, *Adv. Energy Mater.* **2022**, *12*, 2102785; b) M. Fichtner, K. Edström, E. Ayerbe, M. Berecibar, A. Bhowmik, I. E. Castelli, S. Clark, R. Dominko, M. Erakca, A. A. Franco, A. Grimaud, B. Horstmann, A. Latz, H. Lorrmann, M. Meeus, R. Narayan, F. Pammer, J. Ruhland, H. Stein, T. Vegge, M. Weil, *Adv. Energy Mater.* **2022**, *12*, 2102904.
[10] Y. Wang, Z. Wu, F. M. Azad, Y. Zhu, L. Wang, C. J. Hawker, A. K. Whittaker, M. Forsyth, C. Zhang, *Nat. Rev. Mater.* **2024**, *9*, 119–133.
[11] a) Y.-K. Liu, C.-Z. Zhao, J. Du, X.-Q. Zhang, A.-B. Chen, Q. Zhang, *Small* **2023**, *19*, 2205315; b) N. von Aspern, G.-V. Röschenthaler, M. Winter, I. Cekic-Laskovic, *Angew. Chem. Int. Ed.* **2019**, *58*, 15978–16000.
[12] a) N. Xu, J. Shi, G. Liu, X. Yang, J. Zheng, Z. Zhang, Y. Yang, *J. Power Sources Adv.* **2021**, *7*, 100043; b) H. Adenusi, G. A. Chass, S. Passerini, K. V. Tian, G. Chen, *Adv. Energy Mater.* **2023**, *13*, 2203307.
[13] a) T. C. Nirmale, N. D. Khupse, R. S. Kalubarme, M. V. Kulkarni, A. J. Varma, B. B. Kale, *ACS Sustainable Chem. Eng.* **2022**, *10*, 8297–8304; b) C. Amanchukwu, Z. Yu, X. Kong, J. Qin, Y. Cui, Z. Bao, *J. Am. Chem. Soc.* **2020**, *142*, 7393–7403; c) S. Fang, Z. Zhang, Y. Jin, L. Yang, S.-i. Hirano, K. Tachibana, S. Katayama, *J. Power Sources* **2011**, *196*, 5637–5644.
[14] a) M. L. Ferreira, N. S. M. Vieira, P. J. Castro, L. F. Vega, J. M. M. Araujo, A. B. Pereiro, *J. Mol. Liq.* **2022**, *359*, 119285; b) M. L. Ferreira, M. J. Pastoriza-Gallego, J. M. M. Araújo, J. N. Canongia Lopes, L. P. N. Rebelo, M. M. Piñeiro, K. Shimizu, A. B. Pereiro, *J. Phys. Chem. C* **2017**, *121*, 5415–5427.
[15] a) S. M. V. Nicole, L. F. Margarida, J. C. Paulo, M. M. A. João, B. P. Ana, in Ionic Liquids (Ed.: S. M. S. Murshed), IntechOpen, Rijeka, **2021**, pp. 23-47; b) P. Liu, Y. Rao, H. Wang, X. Li, X. Wang, M. Yu, Y. Li, Z. Yue, F. Wu, S. Fang, *Batter. Supercaps* **2024**, *7*, e202300353; c) Q. Liu, C.-W. Hsu, T. L. Dzwiniel, K. Z. Pupek, Z. Zhang, *Chem. Commun.* **2020**, *56*, 7317–7320.
[16] a) W. Qian, J. Texter, F. Yan, *Chem. Soc. Rev.* **2017**, *46*, 1124–1159; b) M. Watanabe, M. L. Thomas, S. Zhang, K. Ueno, T. Yasuda, K. Dokko, *Chem. Rev.* **2017**, *117*, 7190–7239; c) M. Forsyth, L. Porcarelli, X. Wang, N. Goujon, D. Mecerreyes, *Acc. Chem. Res.* **2019**, *52*, 686–694.
[17] H.-B. Han, S.-S. Zhou, D.-J. Zhang, S.-W. Feng, L.-F. Li, K. Liu, W.-F. Feng, J. Nie, H. Li, X.-J. Huang, M. Armand, Z.-B. Zhou, *J. Power Sources* **2011**, *196*, 3623–3632.
[18] N. Sánchez-Ramírez, B. D. Assresahegn, D. Bélanger, R. M. Torresi, *J. Chem. Eng. Data* **2017**, *62*, 3437–3444.
[19] a) J. Leys, M. Wübbenhorst, C. P. Menon, R. Rajesh, J. Thoen, C. Glorieux, P. Nockemann, B. Thijs, K. Binnemans, S. Longuemart, *J. Chem. Phys.* **2008**, *128* (6), 064509; b) J. R. Sangoro, F. Kremer, *Acc. Chem. Res.* **2012**, *45*, 525–532.
[20] a) X. Wang, Y. Chi, T. Mu, *J. Mol. Liq.* **2014**, *193*, 262–266; b) H. Tokuda, K. Hayamizu, K. Ishii, M. A. B. H. Susan, M. Watanabe, *J. Phys. Chem. B* **2005**, *109*, 6103–6110.
[21] H. Matsumoto, H. Sakaebe, K. Tatsumi, M. Kikuta, E. Ishiko, M. Kono, *J. Power Sources* **2006**, *160*, 1308–1313.
[22] C. A. Angell, Y. Ansari, Z. Zhao, *Faraday Discuss.* **2012**, *154*, 9–27.
[23] a) K. R. Harris, *J. Phys. Chem. B* **2019**, *123*, 7014–7023; b) D. R. MacFarlane, M. Forsyth, E. I. Izgorodina, A. P. Abbott, G. Annat, K. Fraser, *Phys. Chem. Chem. Phys.* **2009**, *11*, 4962–4967.
[24] W. Xu, E. I. Cooper, C. A. Angell, *J. Phys. Chem. B* **2003**, *107*, 6170–6178.
[25] L. N. Patro, O. Burghaus, B. Roling, *Phys. Rev. Lett.* **2016**, *116*, 185901.
[26] C. S. Kang, X. Zhang, D. R. MacFarlane, *J. Phys. Chem. C* **2018**, *122*, 24550–24558.
[27] a) Z. P. Rosol, N. J. German, S. M. Gross, *Green Chem.* **2009**, *11*, 1453–1457; b) J. Asenbauer, N. Ben Hassen, B. D. McCloskey, J. M. Prausnitz, *Electrochim. Acta* **2017**, *247*, 1038–1043; c) J. Tong, S. Wu, N. von Solms, X. Liang, F. Huo, Q. Zhou, H. He, S. Zhang, *Front. Chem.* **2020**, *7*, 945.
[28] A. Warrington, L. A. O'Dell, O. E. Hutt, M. Forsyth, J. M. Pringle, *Energy Adv.* **2023**, *2*, 530–546.
[29] a) F. L. Celso, G. B. Appetecchi, C. J. Jafta, L. Gontrani, J. N. C. Lopes, A. Triolo, O. Russina, *J. Chem. Phys.* **2018**, *148*, 193816; b) F. L. Celso, G. Appetecchi, E. Simonetti, U. Keiderling, L. Gontrani, A. Triolo, O. Russina, *J. Mol. Liq.* **2019**, *289*, 111110; c) A. Triolo, O. Russina, B. Fazio, R. Triolo, E. Di Cola, *Chem. Phys. Lett.* **2008**, *457*, 362–365.
[30] G. M. C. Silva, M. J. Beira, P. Morgado, L. C. Branco, P. J. Sebastiao, J. N. Canongia Lopes, E. J. M. Filipe, *J. Mol. Liq.* **2022**, *367*, 120506.
[31] a) F. Lundin, A. I, dström, P. Falus, L. Evenäs, S. Xiong, A. Matic, *J. Phys. Chem. C* **2022**, *126*, 16262–16271; b) X. Liu, M. Zarrabeitia, A. Mariani, X. Gao, H. M. Schuetz, S. Fang, T. Bizien, G. A. Elia, S. Passerini, *Small Methods* **2021**, *5*, 2100168.
[32] J. Liu, X. Yan, L. Gao, L. Hu, X. Wu, Y. Dai, X. Ruan, G. He, *J. Membr. Sci.* **2019**, *581*, 82–92.

Manuscript received: June 21, 2024
Accepted manuscript online: July 3, 2024
Version of record online: September 3, 2024